Int. J. Heat Mass Transfer. Vol. 28, No. 1, pp. 155–163, 1985
Printed in Great Britain

0017-9310/85 $3.00 + 0.00

Experimental investigation of conjugate natural convection heat transfer from a horizontal isothermal cylinder with a nonisothermal longitudinal plate fin at various angles

A. K. TOLPADI and T. H. KUEHN
Department of Mechanical Engineering, University of Minnesota,* Minneapolis, MN 55455-0111, U.S.A.

(*Received* 17 *October* 1983 *and in revised form* 17 *May* 1984)

Abstract—Steady laminar natural convection heat transfer from a horizontal isothermal cylinder in water with a single nonisothermal longitudinal plate fin at various angles is studied experimentally. Results are obtained at a Rayleigh number of approximately 4.0×10^5 with a fin length to cylinder diameter ratio of 0.2 and a Prandtl number near 5. Local fin temperatures and heat transfer from the fin and cylinder are obtained using a Mach–Zehnder interferometer. Overall heat transfer measurements are made from thermocouple and multimeter data for comparison. The total heat transfer does not change significantly from the bare cylinder value. The plume separation shifts from above the heated cylinder to the fin tip when the fin is within 50° of the upward vertical position.

INTRODUCTION

NATURAL convection from finned heat exchangers is a popular area of current research. Applications include space heating, batch process heating and sensible and latent thermal storage. Both experimental and theoretical studies have been performed utilizing isothermal fins. The situation becomes more complicated when the fins are nonisothermal, as they are in liquids, because the fin conduction and natural convection are coupled. Furthermore, this problem is challenging because it involves the interaction of flows between the fin and its base.

Past experimental work on natural convection from finned surfaces considered isothermal fin arrays. Starner and McManus [1] presented average heat transfer coefficients for natural convection from rectangular fin arrays positioned with the base vertical, 45° from the vertical and horizontal while dissipating heat to air. The fins were isothermal and each of the variables, fin spacing, fin height and base orientation, were found to affect the total heat transfer. Welling and Wooldridge [2] considered isothermal fins on vertical surfaces and found that for a given temperature difference there exists an optimum fin height to fin channel width ratio for maximum total heat transfer. Harahap and McManus [3] obtained mean heat transfer coefficients on fin arrays in air with a horizontal base and proposed an overall heat transfer correlation that included three geometry terms. Jones and Smith [4] studied the cooling of isothermal fin arrays on a horizontal base by measuring local heat transfer coefficients with a Mach–Zehnder interferometer. The mean heat transfer coefficient was correlated using the Grashof number based on the fin spacing.

The work described above provides only mean heat transfer coefficients on isothermal fins. Some local natural convection heat transfer data on isothermal fins have also been published. Aihara [5, 6] experimentally studied vertical isothermal fin arrays in air and separated the fin and base plate heat transfers. Extending this work, Aihara [7] considered nonisothermal fins and presented empirical correlations for the effects of fin geometry, thermal conductivity and temperature on the mean heat transfer. Experimental measurements were given for comparison. Sparrow and Bahrami [8] performed experiments to determine mass transfer distributions on the faces of simulated isothermal circular fins fixed to a horizontal adiabatic tube. A napthalene sublimation mass transfer approach was used which suggested that the highest coefficients occur at the fin periphery while the lowest occur at the fin base.

Some local heat transfer measurements have been made on transverse finned tubes in forced convection. Wong [9] used the napthalene sublimation technique to obtain local mass transfer coefficients on concentrically and eccentrically finned cylinders in air. Jones and Russell [10] performed similar work but measured local heat transfer coefficients using a transient technique, i.e. by suddenly injecting the model into an air stream and recording the local temperature variation.

Some systematic studies of boundary layer interaction between a natural convection fin and its base have been made recently. Sparrow and his coworkers conducted experiments to investigate the natural convection heat transfer characteristics of a short isothermal cylinder [11] and arrays of such cylinders [12] attached to an equi-temperature plate.

* This work was done when both authors were at Iowa State University, Ames, Iowa.

NOMENCLATURE

C_F	fin conduction parameter, $k_F t_F/2kD$
D	cylinder diameter
h	local convective heat transfer coefficient
k	fluid thermal conductivity
k_F	fin thermal conductivity
L	fin length
L_F	dimensionless fin length, L/D
Nu	Nusselt number, hD/k
Pr	Prandtl number
q_c	cylinder local heat flux, $h(T_c - T_\infty)$
q_F	fin local heat flux, $h(T_F - T_\infty)$
r	radial coordinate
Ra	Rayleigh number based on cylinder diameter
t_F	fin thickness
T	temperature.

Greek symbols

Δ	increment
θ	angle measured clockwise from top.

Superscript

$\bar{}$	mean.

Subscripts

c	cylinder
F	fin
T	total
∞	infinite fluid.

The effects of cylinder dimensions, intercylinder spacing, positions of the cylinders on the plate, and Rayleigh number were studied. Kwon and Kuehn [13] theoretically analyzed conjugate heat transfer by steady laminar natural convection from an infinitely long vertical conducting fin attached below a heated isothermal cylinder and developed heat transfer correlations that included the fin–cylinder boundary layer overlap. Kwon *et al.* [14] extended this work to the case of a short vertical fin. The same numerical technique was used, but optical data were obtained to verify the numerical results.

The configuration considered here is a horizontal isothermal cylinder with a single longitudinal conducting plate fin attached at an arbitrary angle. It is also the limiting case of a helical fin with a long pitch. This problem is governed by five dimensionless parameters—Rayleigh number Ra; Prandtl number Pr; fin conduction parameter C_F; dimensionless fin length L_F; and fin orientation θ. The effect of a fixed length fin at different orientations is studied.

Local heat transfer data for the finned cylinder were obtained using a Mach–Zehnder interferometer with the fin at five different positions—vertically downwards, 45° from the bottom, horizontal, 45° from the top and vertically upwards. All data were obtained at $Ra \approx 4 \times 10^5$, $Pr \approx 5$, $L_F = 0.20$ and $C_F \approx 0.6$. Some simple flow visualization studies were also performed to seek an explanation for the heat transfer distributions observed.

APPARATUS

A plain cylinder and a finned cylinder were designed and constructed for use in a Mach–Zehnder interferometer. A cross-sectional view of the slotted cylinder assembly is given in Fig. 1. The thick-walled copper cylinders were machined from a solid copper rod to provide isothermal surface conditions. A 0.63 cm diameter hole was drilled axially in the center to hold a 68 Ω electric resistance heater and a 1.27 cm diameter threaded hole was machined at each end for Plexiglass endcaps. Eight equally spaced holes were drilled axially from one end within 2 mm of the surface to contain copper–constantan thermocouple junctions. These junctions were electrically isolated and connected in series to eight additional junctions immersed in the surrounding fluid to form a thermopile for greater temperature difference sensitivity. An axial slot, 0.526 cm deep and 0.115 cm wide, was machined in one of the cylinders for holding an axial plate fin. The fin was cut from 0.112 cm thick V2A stainless steel plate with its

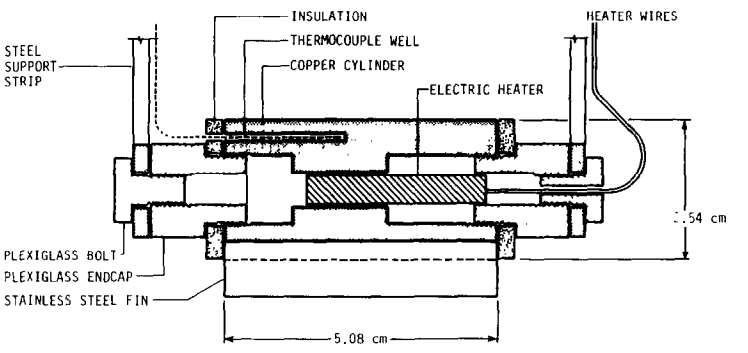

FIG. 1. Cross-sectional view of the finned cylinder.

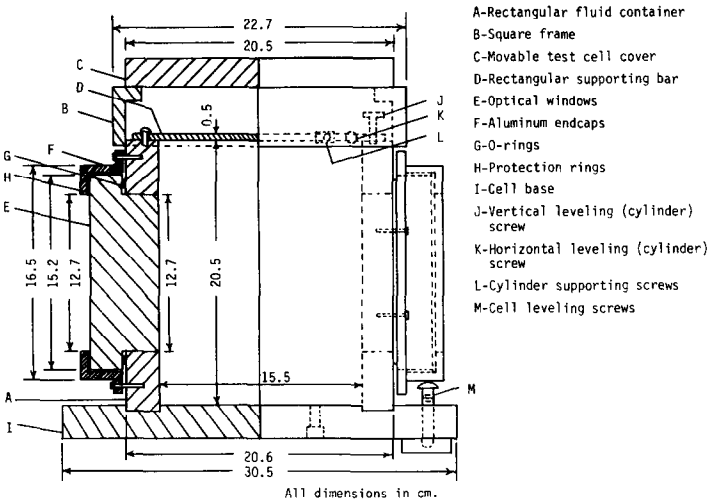

FIG. 2. Elevation of test cell, half in section.

length equal to that of the cylinder. The value of C_F was approximately 0.6 when the fin was immersed into water at room temperature. The height was selected such that the length of the fin projecting beyond the cylinder was approximately one-fifth of the diameter when the fin was press fitted into the slot. This fin length was previously found to provide the largest heat transfer per unit length of fin when $C_F \approx 0.6$ and the fin is below the cylinder [14]. Expanded polystyrene disks were mounted on each end of the cylinders to minimize end losses. Each cylinder was supported by two thin steel strips each welded to a washer and secured by a bolt that enabled the entire cylinder assembly to be rotated about its axis.

A test cell was constructed of 2.54 cm thick Plexiglas to contain the distilled water surrounding the cylinder. The inside dimensions were 15.5 cm × 15.5 cm × 20.5 cm high. A schematic cross-section is given in Fig. 2. Two custom-made 5.08 cm thick optical grade windows were mounted on opposite sides of the cell for interferometric measurements. The windows were stepped so that the inside surface was flush with the inside of the test cell and the flange was used to provide compression on a rubber gasket. The cell was attached to a Plexiglas base plate which had three leveling screws. A square Plexiglas frame mounted on top had holes for bringing out the thermocouple and heater wires. A rectangular Plexiglas bar was mounted on top of the test cell from which the support strips for the cylinder assembly were suspended. Two screws on one end facilitated adjustments both in the vertical and horizontal planes. The cell was covered by a movable Plexiglas cover.

Overall measurements were made using digital multimeters that recorded the heater power input and a millivolt potentiometer that measured the thermocouple emf. Optical measurements were made by placing the test cell with the cylinder into one of the arms of a modified Mach–Zehnder interferometer that used a 2 mW He–Ne laser as the light source. All components of the interferometer were positioned so that the light beam was incident on each at an angle of 30° rather than 45° as in a conventional design. By using 30° a wider beam can be obtained. The test cell and all components of the interferometer except the first paraboloidal mirror were placed on an optical table with air bag suspension. The mirror was placed on a separate table with a small d.c. motor attached to the back. The motor caused the mirror to vibrate slightly and eliminated any background fringes giving a clean picture of the 'true' fringes around the cylinder.

PROCEDURE

Before any runs were made, the optical table was leveled by inflating the air bags and then the water-filled test cell was leveled on the table using the leveling screws. The interferometer was adjusted to an infinite fringe setting with the test cell placed in the measuring leg. The adjustment technique is quite standard and the details may be found in [15]. Next, the cylinder assembly was lowered into the test cell, rotated to the proper fin angle, and aligned with the light beam using the adjusting screws on the support bar. The camera was focused on the center of the cylinder and power to the heater was turned on.

A problem that was encountered in the test cell was stratification and vortex ring formation [16]. Theoretically, the fluid should be infinite in extent but the actual test cell is finite. If the cell cover is completely closed, the warm fluid rising to the surface cannot dissipate the heat causing the outer fringes to spread out horizontally indicating stratification. To facilitate heat removal from the sides of the cell, the cell was left uninsulated. On the other hand, if the cover is completely removed, the rising laminar plume interacts with the air interface producing a turbulent mixing layer in which vortex rings are formed that penetrate into the underlying fluid causing the fringe pattern to become unstable. Hence, a balance point of the test cell

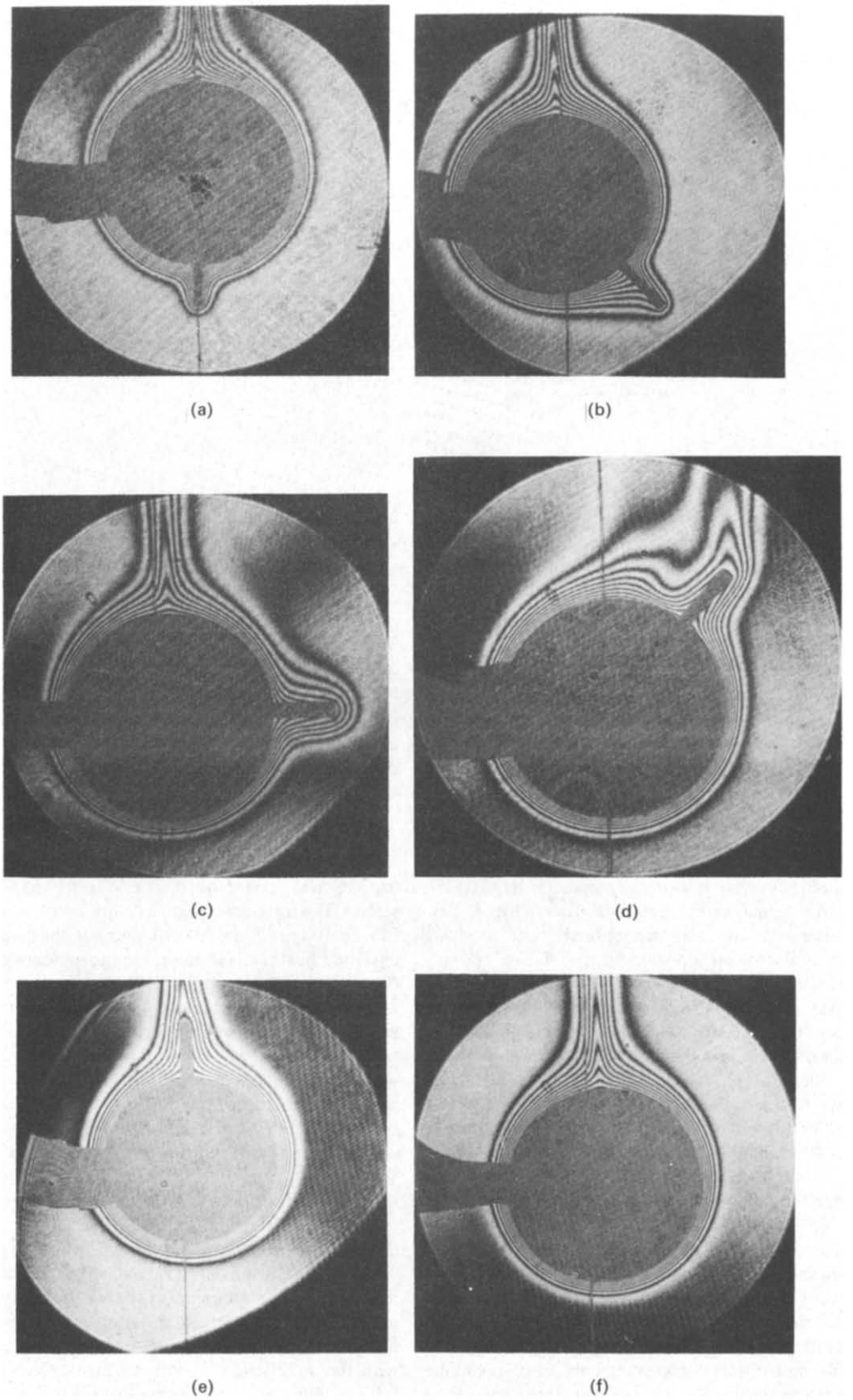

FIG. 3. Interferograms with the fin at different angles in water, $L_F = 0.20$, $C_F = 0.60$.

cover had to be found to obtain a good stable fringe pattern with no stratification.

Interferograms were recorded on 35 mm fine grain film using a 135 mm telephoto lens. Fringe positions were measured from the film negatives under a tool maker's microscope that gave the fluid radial temperature profiles, the fin temperature distribution and local heat flux from the cylinder and fin. The fringe data reduction procedure was essentially a modification of the technique used by Kuehn and Goldstein [17] that included corrections for first and second order refraction errors, fringe position errors due to refraction, and a correction for end effects. All fluid properties were evaluated at the arithmetic mean temperature between the cylinder and bulk fluid. A slightly different procedure was used in the calculation of the local fin temperature. The fin surface being nonisothermal, the temperature corresponding to the outermost fringe was set equal to the surrounding fluid temperature and by using a reversed calculation procedure, the local fin temperature was computed.

The finite-length cylinder causes conduction losses to occur from the ends which must be accounted for. The measured power input to the heater must be corrected to get the actual convective power. To do this, the Nusselt numbers for a free cylinder based on the measured power input were compared to a heat transfer correlation [18]. They were naturally different and by back-calculating, the correction factor was estimated. The main source of error in the overall measurements is in the determination of the cylinder to fluid temperature difference. The error in the voltage measurement by the millivolt potentiometer is 4.5%. With this, the maximum error in the Rayleigh and mean Nusselt numbers are 5% and 5.5% respectively. Misalignment of the cylinder is the largest source of error in the optical measurements, as it results in the loss of some inner fringes causing an error in the determination of the surface position and surrounding temperature gradient. If the cylinder is well aligned, then the chief source of error is in reading the fringes from the interferograms. This caused a maximum error of 2% in the Rayleigh number and 6% in the local and mean Nusselt numbers.

After all the optical data were taken, some simple qualitative flow visualization studies were performed. Some impurities were added to the water and the flow patterns near the finned cylinder were observed by illuminating the test cell from one side. Complete details of the instrumentation and experimental procedure are available in [19].

RESULTS

The amount of experimental data obtained from each interferogram is quite overwhelming so that only six different runs are discussed here. The results for different lengths of downward projecting fins were given in [14]. Comparison with corresponding numerical results showed good agreement. The thrust

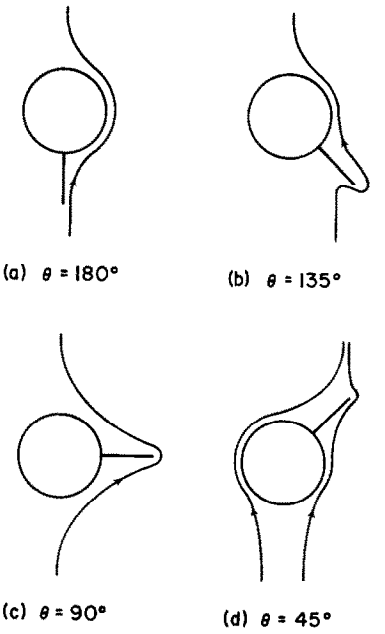

FIG. 4. Qualitative sketches of pathlines with the fin at different angles.

of this study is to analyze the heat transfer with a fin at other orientations. The fin position varied with angle from directly below to directly above the heated cylinder.

Interferograms of each of the five fin orientations studied along with an interferogram of the free cylinder are shown in Fig. 3. Sketches of some of the pathlines observed at each orientation of the fin are shown in Fig. 4. Although these are qualitative, they do provide useful information in explaining the heat transfer results. There are considerable differences in the flow between the various fin positions. The most interesting aspect is the change in the structure of the plume that occurs when the fin is placed near the top symmetry line. From $\theta_F = 180°$ to $\theta_F \approx 65°$, the plume rises above the center of the cylinder and is not affected by the presence of the fin. Between $\theta_F = 0$ and 50°, the plume shifts completely to the region above the fin tip. A zone of transition exists between $\theta_F \approx 50°$ and 65°, when two plumes are formed, one leaving the top of the cylinder, the other from the fin tip with a possible recirculatory zone between the two plumes. The two plumes combine some distance above the cylinder.

Fringe measurements indicated the temperature to be uniform across the fin, meaning the fin temperature distribution is nearly one-dimensional. However, the differences in the fringe spacing on either side of the fin, when not positioned vertically, show that the local heat flux distribution is different on each side.

The fin temperature distribution at each fin position is shown in Fig. 5. The fin temperatures generally increase as the orientation of the fin is changed from the vertically downward ($\theta_F = 180°$) to the vertically upward position. This is because the surrounding fluid

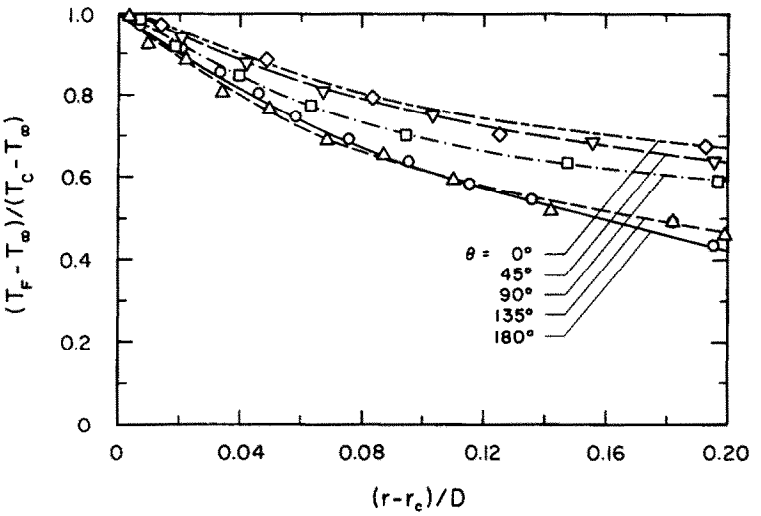

FIG. 5. Temperature distribution along the fin at various orientations, $L_F = 0.20$, $C_F = 0.60$, $Pr = 5.2$.

is warmest in the plume region causing the fin to have the highest temperature when placed above the cylinder. The fin temperature is lowest when it is positioned downwards because of the low temperature fluid in that region and the large convective heat transfer coefficient.

Figure 6 shows the local Nusselt number variation along the surfaces of the fin (both above and below it when the fin is not vertical) at various orientations. The average fin Nusselt number decreases as the fin orientation is changed from the vertically downward to the upward position. This is to be expected because the fin when positioned above the cylinder lies in a region of small temperature gradients causing the heat transfer coefficient to decrease. This decreased heat transfer coefficient results in a higher fin temperature which explains the increasing fin temperatures shown in Fig. 5. When oriented 135° from the top, the heat transfer coefficient on the upper surface of the fin is much higher than below. This can also be observed in the interferogram in Fig. 3(b) where the fringe spacing normal to the fin surface is much smaller above the fin than below. Flow visualization showed the fluid to be moving towards the cylinder above the fin but moving away from the cylinder below (see Fig. 4(b)). The velocity above the fin was also higher which explains the higher heat transfer coefficient there. However, with the fin mounted horizontally, the velocity along both sides of the fin was found to be roughly of the same magnitude but opposite in direction which explains the nearly equal heat transfer coefficient on both sides.

It is of interest to compare the fin results at $\theta_F = 180°$ on Figs. 5 and 6 with those of Sparrow and Acharya [20]. No fin–cylinder boundary layer interaction is present in [20] and the fin is treated as having zero thickness unlike the present fin. The fin temperature distributions show qualitative agreement but the local Nusselt number distributions are considerably different. The discrepancy is attributed to the two differences mentioned above.

The local Nusselt number distributions around the isothermal cylinder at different fin orientations are shown in Fig. 7 which corresponds to the interferograms given in Fig. 3. The free cylinder data are shown on each for comparison. Whenever there was vertical symmetry, measurements were made only on one side of the cylinder. For each case, it may be observed that the local heat transfer distribution on the finned cylinder agrees well with the free cylinder distribution except near the fin, where the presence of

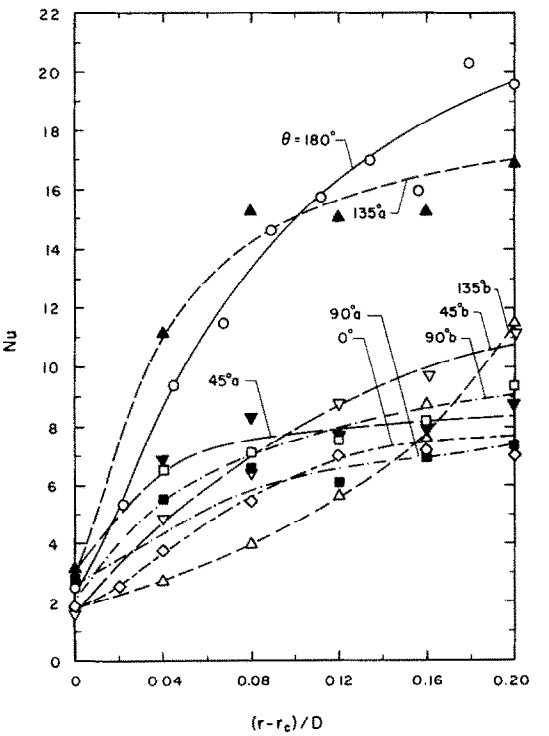

FIG. 6. Local Nusselt number distribution along the fin at various orientations, $L_F = 0.20$, $C_F = 0.60$, $Pr = 5.2$ (a = above, b = below).

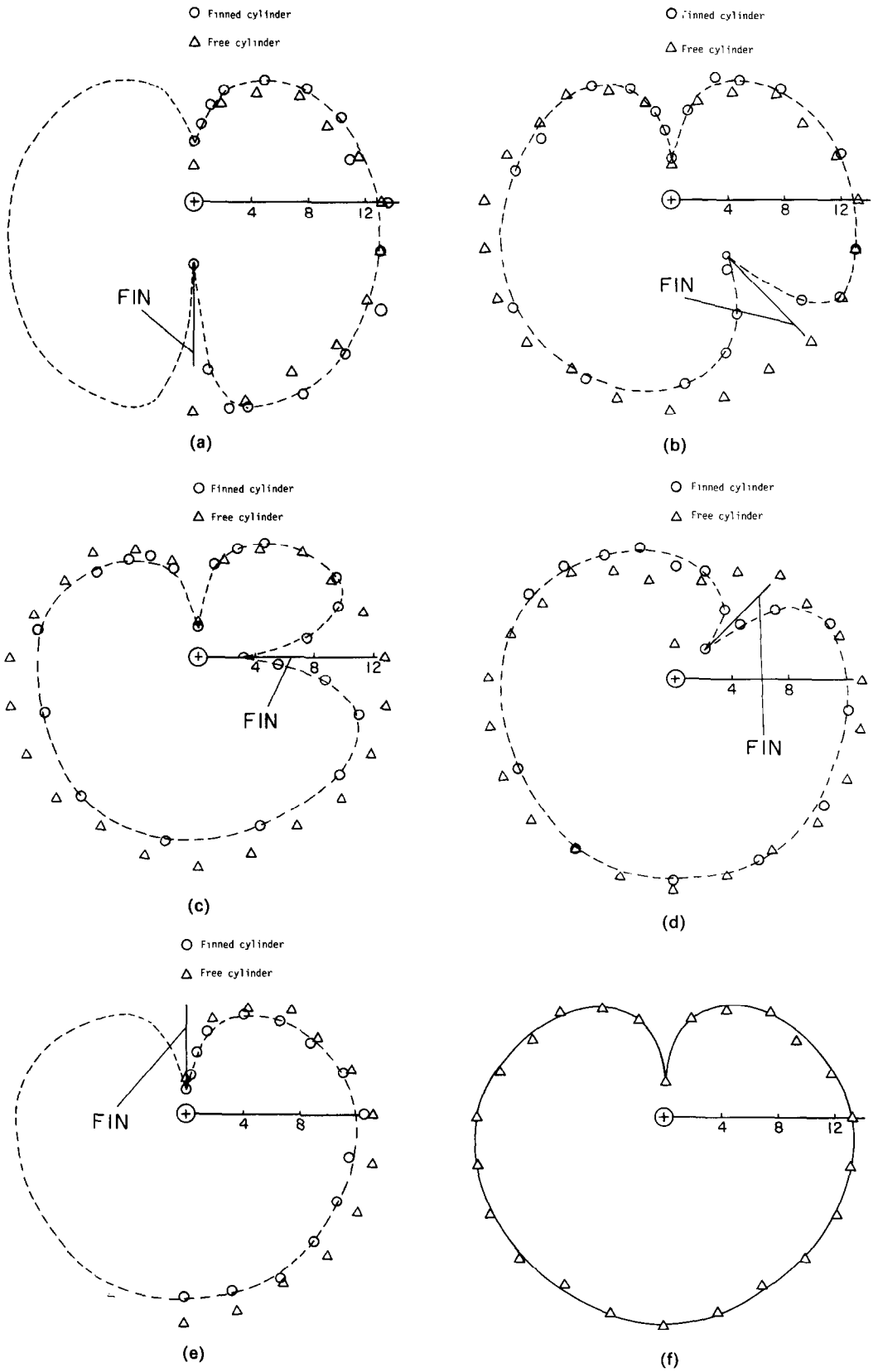

FIG. 7. Nusselt number distribution around the cylinder with the fin at various orientations, $L_F = 0.20$, $C_F = 0.60$, $Pr = 5.2$.

Table 1. Optical mean heat transfer measurements for a cylinder with a single longitudinal fin positioned at different orientations, $C_F = 0.60$, $L_F = 0.20$

θ_F (degrees)	$Ra \times 10^5$	Pr	T_∞ (°C)	$T_c - T_\infty$ (°C)	$\frac{\bar{T}_F - T_\infty}{T_c - T_\infty}$	$\overline{Nu}_F$ (± 0.1)	$\overline{Nu}_C$ (± 0.7)	$\overline{Nu}_T$ (± 0.8)	$\overline{Nu}_T/Ra^{0.25}$ (± 0.04)
180	4.29	5.2	32.2	0.94	0.66	1.8	11.2	13.0	0.51
135	3.91	5.2	31.7	0.89	0.66	2.0	10.9	12.9	0.52
90	3.26	5.2	32.0	0.73	0.73	1.3	10.4	11.7	0.49
45	3.61	5.2	31.8	0.82	0.78	1.1	11.8	12.9	0.53
0	3.71	5.2	31.8	0.84	0.80	1.0	11.5	12.5	0.50
free cylinder	3.50	5.2	32.2	0.79	—	—	12.3	12.3	0.50

the fin thermal boundary layer reduces the cylinder local heat transfer considerably. With the fin placed vertically upwards in the plume, the cylinder Nusselt number distribution is nearly identical to that of the free cylinder as evidenced in Fig. 7(e). However, when the fin is placed 45° from the top, the departure from the free cylinder heat transfer distribution occurs over a larger region near the fin because of the shift in the position of the plume separation.

The optically computed mean heat transfer results are summarized in Table 1. The table shows an integration of all the data presented above. The fin heat transfer is an integration of the product of the results shown in Figs. 5 and 6. As the fin is rotated upwards, its mean temperature increases. The fin mean temperature is essentially invariant when $\theta_F \geqslant 135°$. The fin mean heat transfer coefficient tends to decrease as θ_F changes from 180° to 0°. The presence of the fin causes the cylinder mean heat transfer to be reduced below that of the free cylinder in all cases with larger decreases when the fin is near the bottom. The fin and cylinder mean heat transfer trends are opposite with respect to fin orientation. Therefore, the combined fin and cylinder heat transfer results, $\overline{Nu}_T$, are nearly uniform and not significantly different from the free cylinder value.

The last column in Table 1 shows the total fin and cylinder heat transfer divided by $Ra^{0.25}$ which should remove any dependence on the Rayleigh number leaving the fin orientation as the sole variable. The results show very little change from the free cylinder value indicating that the fin does not have a significant effect on the total heat transfer for any orientation studied here.

CONCLUSIONS

1. The total heat transfer by natural convection from a heated cylinder with a short longitudinal fin does not change significantly from the free cylinder value for any fin orientation.

2. The plume separation shifts from above the cylinder to the fin tip when the fin is inclined from the upward vertical position $0 \leqslant \theta_F \leqslant 50°$. This may be useful in designing arrays of finned tubes.

3. The local and mean heat transfer coefficients on the two sides of a fin are considerably different when the fin is not vertical.

Acknowledgement—This work was supported by the National Science Foundation through grant CME-8003498.

REFERENCES

1. K. E. Starner and H. N. McManus An experimental investigation of free-convection heat transfer from rectangular fin arrays, *ASME J. Heat Transfer* **85,** 273–278 (1963).
2. J. R. Welling and C. B. Wooldridge, Free-convection heat transfer coefficients from rectangular vertical fins, *ASME J. Heat Transfer* **87,** 439–444 (1965).
3. F. Harahap and H. N. McManus, Natural convection heat transfer from horizontal rectangular fin arrays, *ASME J. Heat Transfer* **89,** 32–38 (1967).
4. C. D. Jones and L. F. Smith, Optimum arrangement of rectangular fins on horizontal surfaces for free-convection heat transfer, *ASME J. Heat Transfer* **92,** 6–10 (1970).
5. T. Aihara, Natural convection heat transfer from vertical rectangular fin arrays—Part 1, *Trans. JSME* **34,** 915–926 (1968).
6. T. Aihara, Natural convection heat transfer from vertical rectangular fin arrays—Part 3, *Bull. JSME* **13,** 1192–1200 (1970).
7. T. Aihara, Natural convection heat transfer from vertical rectangular fin arrays—Part 4, *Bull. JSME* **14,** 818–828 (1971).
8. E. M. Sparrow and P. A. Bahrarmi, Experiments on natural convection heat transfer on the fins of a finned horizontal tube, *Int. J. Heat Mass Transfer* **23,** 1555–1560 (1980).
9. P. W. Wong, Mass and heat transfer from circular finned cylinders, *JIHVE* **34,** 1–23 (1966).
10. T. V. Jones and C. M. B. Russell, Heat transfer distribution on annular fins, ASME Paper No. 78-HT-30 (1978).
11. E. M. Sparrow and G. M. Chrysler, Natural convection heat transfer coefficients for a short horizontal cylinder attached to a vertical plate, *ASME J. Heat Transfer* **103,** 630–637 (1981).
12. E. M. Sparrow, D. S. Cook and G. M. Chrysler, Heat transfer by natural convection from an array of short, wall-attached horizontal cylinders, *ASME J. Heat Transfer* **104,** 125–131 (1982).
13. S. S. Kwon and T. H. Kuehn, Conjugate natural convection heat transfer from a horizontal cylinder with a long vertical longitudinal fin, *Numerical Heat Transfer* **6,** 85–102 (1983).
14. S. S. Kwon, T. H. Kuehn and A. K. Tolpadi, Conjugate natural convection heat transfer from a short vertical longitudinal fin below a heated horizontal cylinder, ASME Paper No. 83-HT-100 (1983).
15. W. Hauf and U. Grigull, Optical methods in heat transfer, *Advances in Heat Transfer* Vol. 6, pp. 133–366, Academic Press (1970).
16. F. P. Incropera and M. A. Yaghoubi, Buoyancy driven

flows originating from heated cylinders submerged in a finite water layer, *Int. J. Heat Mass Transfer* **23**, 269–278 (1980).
17. T. H. Kuehn and R. J. Goldstein, An experimental and theoretical study of natural convection in the annulus between horizontal concentric cylinders, *J. Fluid Mech.* **74**, 695–719 (1976).
18. T. H. Kuehn and R. J. Goldstein, Correlating equations for natural convection heat transfer between circular cylinders, *Int. J. Heat Mass Transfer* **10**, 1127–1134 (1976).
19. A. K. Tolpadi, Experimental and numerical study of conjugate natural convection heat transfer from fins, M.S. Thesis, Iowa State University, Ames, Iowa (1983).
20. E. M. Sparrow and S. Acharya, A natural convection fin with a solution-determined nonmonotonically varying heat transfer coefficient, *ASME J. Heat Transfer* **103**, 218–225 (1981).

ETUDE EXPERIMENTALE DE LA CONVECTION THERMIQUE NATURELLE AUTOUR D'UN CYLINDRE ISOTHERME, HORIZONTAL AVEC UNE AILETTE PLANE LONGITUDINALE A ANGLES VARIES

Résumé—On étude expérimentalement la convection thermique naturelle, laminaire et stationnaire autour d'un cylindre isotherme hotizontal dans l'eau, avec une ailette longitudinale unique à angles variés. Des résultats sont obtenus à un nombre de Rayleigh de 4×10^5 environ, avec une hauteur d'aillette 0,2 fois le diamètre du cylindre et un nombre de Prandtl proche de 5. Les températures locales de l'ailette et le transfert thermique sur l'ailette et le cylindre sont obtenus à l'aide d'un interféromètre Mach–Zehnder. Les mesures de transfert thermique global sont faites à partir des données des thermocouples et d'un multimètre pour comparaison. Le transfert thermique total ne change pas beaucoup à partir du cylindre nu. La séparation du panache se déplace du sommet du cylindre chauffé vers le sommet de l'ailette lorsque l'ailette est située à l'intérieur d'un angle de 50° à partir de la position verticale.

EXPERIMENTELLE UNTERSUCHUNG DER WÄRMEÜBERTRAGUNG DURCH NATÜRLICHE KONVEKTION VON EINEM HORIZONTALEN ISOTHERMEN ZYLINDER MIT EINER NICHTISOTHERMEN IN LÄNGSRICHTUNG UNTER VARIABLEM WINKEL ANGEBRACHTEN PLATTENRIPPE

Zusammenfassung—Die Wärmeübertragung durch stationäre, laminare natürliche Konvektion von einem horizontalen isothermen Zylinder an Wasser wird experimentell untersucht. An dem Zylinder ist in Längsrichtung eine einzige Plattenrippe unter variablem Winkel angegeben. Es wurden Ergebnisse bei einer Rayleighzahl von ungefähr $4{,}0 \times 10^5$ mit einem Verhältnis von Rippenlänge zu Zylinderdurchmesser von 0,2 und einer Prandtlzahl von ungefähr 5 ermittelt. Örtliche Rippentemperaturen und Wärmeübergangsverhältnisse von Rippe und Zylinder wurden durch Verwendung eines Mach–Zehnder Interferometers gemessen. Der Gesamt-Wärmeübergang weicht nicht wesentlich von dem des nackten Zylinders ab. Die Auftriebsfahne wandert von der Oberseite des beheizten Zylinders zu der Rippenspitze, wenn die Rippe um 50° aus der vertikalen Position geneigt wird.

ЭКСПЕРИМЕНТАЛЬНОЕ ИССЛЕДОВАНИЕ СОПРЯЖЕННОГО ЕСТЕСТВЕННО-КОНВЕКТИВНОГО ТЕПЛОПЕРЕНОСА ОТ ГОРИЗОНТАЛЬНОГО ИЗОТЕРМИЧЕСКОГО ЦИЛИНДРА С НЕИЗОТЕРМИЧЕСКИМ ПРОДОЛЬНЫМ ПЛАСТИНЧАТЫМ РЕБРОМ, РАСПОЛОЖЕННЫМ ПОД РАЗНЫМИ УГЛАМИ

Аннотация—Экспериментально изучается стационарный ламинарный естественно-конвективный теплоперенос от помещенного в воду горизонтального изотермического цилиндра с неизотермическим продольным пластинчатым ребром, имеющим различные углы наклона. Результаты получены при числах Рэлея 4.0×10^5, отношении длины ребра к диаметру цилиндра 0.2 и числе Прандтля около 5. Местная температура ребра и теплоотдача ребра и цилиндра определены при помощи интерферометра Маха-Цандера. Для сравнения измерялся общий теплоперенос с помощью термопары и универсального измерительного прибора. Общий теплоперенос не отличался существенно от значений, полученных для цилиндра без ребра. При расположении ребра в пределах 50° от направленного вверх вертикального положения муаровая полоса смещается вниз по нагретому цилиндру к кромке ребра.